Molecular Immunology 109 (2019) 71–80

Contents lists available at ScienceDirect

Molecular Immunology

journal homepage: www.elsevier.com/locate/molimm

The inhibitor of interleukin-3 receptor protects against sepsis in a rat model of cecal ligation and puncture☆

Juntao Hu[a,b,1], Zhanhong Tang[a,1], Jing Xu[b,c], Weiwei Ge[b,d], Qiaohua Hu[e], Fengliang He[b,d], Guanghui Zheng[e], Longyuan Jiang[e], Zhengfei Yang[b,e,*], Wanchun Tang[b,e,*]

[a] Department of Critical Care Medicine, The First Affiliated Hospital of Guangxi Medical University, Nanning, China
[b] Weil Institute of Emergency and Critical Care Research, School of Medicine, Virginia Commonwealth University, Richmond, VA, USA
[c] Department of Emergency, The First Affiliated Hospital of Xi'an Jiaotong University, Xi'an, China
[d] The Second Affiliated Hospital of Anhui Medical University, Anhui Medical University, Hefei, China
[e] Sun Yat-sen Memorial Hospital, Sun Yat-sen University, Guangzhou, China

ARTICLE INFO

Keywords:
IL-3
Cecal ligation and puncture (CLP)
Sepsis

ABSTRACT

Sepsis is defined as a life-threatening organ dysfunction caused by a dysregulated host response to infection. There are multiple cytokines involved in the process of sepsis. As an important upstream cytokine in inflammation, Interleukin-3 (IL-3) plays a crucial role during sepsis, however, its exact role is unclear. The purpose of this study is to discuss the role of IL-3 and its receptor in cecal ligation and puncture (CLP)-induced sepsis in a rat model. The Cluster of Differentiation 123 (CD123, IL-3 receptor alpha chain, IL-3Rac) antibody (anti-CD123) was used to directly target IL-3's receptor and alleviate the effect of IL-3 in the CLP + anti-CD123 group during the early stage of sepsis. CLP was performed in the CLP and CLP + anti-CD123 groups. The time points of observation included 12 h, 24 h, and 5d after the operation. The results showed that the rats in the CLP + anti-CD123 group had lower levels of lactate, serum tumor necrosis factor-α (TNF-α), Interleukin-1β (IL-1β), and Interleukin-6 (IL-6), and also exhibited a higher core temperature, mean arterial pressure (MAP), Oxygenation Index (PO_2/FiO_2), and end-tidal carbon dioxide ($ETCO_2$) and serum Interleukin-10 (IL-10) levels after CLP than those in the CLP group. Additionally, administration of anti-CD123 led to a stable down-regulation of tyrosine phosphorylation of the IL-3 receptor, a decline in phosphorylation of the Janus kinase 2 (JAK2) protein, and the signal transduction and activation of transcription 5 (STAT5) proteins in lung tissues. Meanwhile, the study revealed that treatment of anti-CD123 can markedly attenuate histological damages in lung and kidney tissues, improve sublingual microcirculation, and prolong survival post sepsis. In conclusion, anti-CD123 reduces mortality and alleviates organ dysfunction by restraining the JAK2-STAT5 signaling pathway and reduces serum cytokines in the development of early sepsis in a rat model induced by CLP.

1. Introduction

Sepsis is an organ injury syndrome caused by a dysregulated host response to severe infection, and is a widespread fatal disease characterized by a harmful and uncontrolled pathogenic microorganism infection to the host body (Shankar-Hari et al., 2015; Singer et al., 2016). Based on global estimates, annually there are about 31.5 million sepsis cases, and another 19.4 million cases of severe sepsis worldwide (Fleischmann et al., 2016). The mortality rate of sepsis has recently reached 18.4% (Kaukonen et al., 2014).

Cytokine storm-induced syndrome and microcirculation disturbances are major mechanisms of sepsis (Hawiger et al., 2015; Massey et al., 2018). But a fundamental grasp of the pathophysiology and cytokine network of sepsis is still lacking. Interleukin-3 (IL-3), also named multicolony-stimulating factor (MSF), is derived from the innate response activating factor (IRA) B cells, mast cells, T cells, and eosinophils, and contributes to leukocyte and monocyte production, proliferation, and survival (Weber et al., 2015; Williams et al., 1990). Therefore, monocytes and neutrophils produce IL-1β, IL-6, and tumor necrosis factor-α (TNF-α), the three inflammatory hallmark cytokines constituting the cytokine storm that occurs during septic shock (Angus and van der Poll, 2013; Deutschman and Tracey, 2014; Hotchkiss et al.,

☆ The work was performed at Tang Wanchun Laboratories of Emergency & Critical Care Medicine, Guangzhou, China.

* Corresponding authors at: Sun Yat-sen Memorial Hospital, Sun Yat-sen University, 107 Yan Jiang Xi Road, Guangzhou 510120, China.
E-mail addresses: yangzhengfei@vip.163.com (Z. Yang), wanchun.tang@vcuhealth.org (W. Tang).

[1] Juntao Hu and Zhanhong Tang contributed equally to this study.

https://doi.org/10.1016/j.molimm.2019.03.002
Received 24 November 2018; Received in revised form 1 March 2019; Accepted 1 March 2019
Available online 11 March 2019
0161-5890/

2013; Min et al., 2018). In normal conditions, IL-3 is harmless (Yang et al., 1986). However, under a disease state, high concentrations of IL-3 could lead to a peak in the number of mononuclear cells in circulation after invasive pathogens are detected, and would result in the excessive release of IL-1β, TNF-α, and IL-6, which are the symbols of septic cytokines (Hotchkiss and Sherwood, 2015). Weber et al. (2015) found that mice lacking IL-3 were partially protected from sepsis lethally induced by cecal ligation and puncture (CLP), and considered IL-3 to have a crucial role in the pathogenesis of the early phase of sepsis. Therefore, high plasma IL-3 levels are associated with high mortality even after adjusting for prognostic indicators (Weber et al., 2015). Recently, Min et al. found that elevated plasma IL-3 levels were associated with a high rate of organ failure, and thus a greater risk of mortality in sepsis patients, by using a point-of-care platform for rapid sepsis detection (Min et al., 2018).

Cumulatively, these results confirmed the potential role of IL-3 as a sepsis diagnostic tool and prognosis biomarker. But the mechanism of IL-3 in sepsis has not been fully investigated. IL-3 binds to the IL-3 receptor a chain (known as CD123) to transmit signals, as seen in the effects of IL-3 on leukocyte cell production and survival via the IL-3-CD123 axis. Following IL-3 stimulation, there is an increase in tyrosine phosphorylation and subsequent activation of the receptor-associated protein tyrosine kinase, Janus kinase-2 (JAK2) (Leslie et al., 1996; O'Farrell et al., 1996; Silvennoinen et al., 1993). The activated JAK2 mediates the subsequent phosphorylation of tyrosine residue within the beta-chain of the IL-3 receptor (Duronio et al., 1992; Yi et al., 1993). The phosphotyrosine residue in beta subunits provides docking sites for signal transduction and activation of transcription 5 (STAT5) (Briscoe et al., 1996; Schindler and Darnell, 1995). Phosphorylated STAT5 binds specific DNA elements to activate transcription of target genes (Ihle, 1996), and this signaling accelerates cell proliferation and differentiation, resulting in more inflammatory cytokines. IL-3 may play an important role as an upstream trigger that causes inflammation in early sepsis (Min et al., 2018). Therefore, the IL-3-CD123 axis signal pathway may potentially be a new treatment target for sepsis (Weber et al., 2015).

In this study, we hypothesize that directly targeting the receptor of IL-3 with anti-CD123 in a rat model of the early stage of sepsis induced by CLP will minimize the effect of IL-3 through the IL-3-CD123 axis and improve the prognosis in sepsis and septic shock.

2. Material and methods

2.1. Ethical statement

All animals received humane care in compliance with "Principles of Laboratory Animal Care", enacted by the National Society for Medical Research and Guidelines for the Care and Use of Laboratory Animals formulated by the Institute of Laboratory Animal Resources and produced by the National Institutes of Health (www.aaalac.org; 8th edition; Washington DC, National Academic Press, 2011). The experimental protocol was approved by the committee of the Tang Wanchun Laboratories of Emergency Critical Care Medicine, Sun Yat-Sen Memorial Hospital, Sun Yat-Sen University.

2.2. Chemicals and reagents

The anti-CD123 monoclonal antibody was supplied by ABclonal Biotechnology Co., Ltd. (Wuhan, China). 3,3-diaminobenzidine tetrahydrochloride (DAB) was purchased from Sigma-Aldrich (St. Louis, MO, USA). The antibodies for annexin A1 and β-actin were purchased from Santa Cruz Biotechnology (USA). Secondary antibodies for western blotting were purchased from ABcam Biotechnology Co., Ltd. (Cambridge, MA, USA). Enzyme-linked immunosorbent assay (ELISA) kits were purchased from R&D systems, (Minneapolis, MN, USA). All other chemicals used were of analytical reagent grade.

2.3. Animal preparation

Fifty-five healthy male Sprague-Dawley rats (age 3–4 months; weight 350–450 g) were purchased from Jinan Pengyue Experimental Animal Breeding Co. LTD. (SCXK(Lu)20140007). They were kept four rats to each cage and on a regular 12-hour light and dark cycle (7:00 to 19:00 light period). Food and water were supplied until 12 h prior to the start of the experiment, after which the rats were given only free access to water.

After inhalation of CO_2 for less than 30 s, the animals were given an intraperitoneal injection of pentobarbital (45 mg/kg) to anesthetize, and additional doses (10 mg/kg) were given at intervals of about 1 h, or as needed to maintain anesthesia. The lower abdomens were shaved and disinfected after anesthesia was administered. Tracheas were orally intubated with a 14-gauge (G) cannula mounted on a blunt needle (Abbocath-T; Abbott Hospital Products Division, North Chicago, IL, USA) with a 145 ° angled tip. Spontaneous breathing was maintained. End-tidal carbon dioxide ($ETCO_2$) was continuously measured with an $ETCO_2$ analyzer (BeneView T5, Mindary Bio-Medical Electronics Co. Ltd., Shenzhen, China). Rectal temperature was monitored as core temperature. A polyethylene-50 (PE-50) catheter (Becton Dickinson, Franklin Lakes, NJ, USA) was advanced into the descending aorta from the left femoral artery to measure mean arterial pressure (MAP) and collect blood samples for blood gas analyses, including lactate, oxygenation index (PaO_2/FiO_2), and the concentration of serum cytokines, including IL-1β, IL-3, IL-6, IL-10, and TNF-α. All catheters were flushed intermittently with a 2.5IU /ml crystallized bovine heparin brine. Rats were monitored by a trained professional post-surgery until the end of the experiment. All rats were administrated a 0.05 mg/kg Buprenorphine subcutaneous injection in the loose skin over the shoulder for postoperative analgesia (repeated every 6 h for 2d) (Rittirsch et al., 2009). In order to obtain survival results, rats were monitored for 5 days.

2.4. CLP model

CLP procedures (Rittirsch et al., 2009) were used to induce high grade sepsis in the CLP and CLP + anti-CD123 groups' rats. After anesthesia, a 1 cm midline abdominal incision was made; then intramuscular, fascial, and peritoneal incisions were done, and the cecum was located and exteriorized. The total cecal length was measured from the tip of the ascending cecum to the tip of the descending cecum. The cecum was exteriorized and ligated with 4-0 silk immediately at 75% of its total length and distal to the ileocecal valve without causing an intestinal obstruction. The cecum was then punctured twice with a 20-G needle. After taking out the needle, a small number of feces were extruded. The cecum was repositioned and the abdomen was closed in two layers.

2.5. Experimental protocol

After surgical preparation, the fifty-five rats were randomized into three groups: (1) Sham group (n = 15): the rats underwent laparotomy without puncture or cecal ligation and received an injection of 0.2 ml of vehicle (phosphate buffered saline) via the tail vein at 1 and 6 h respectively post-operation; (2) CLP group (n = 20): the rats underwent CLP and received an injection of 0.2 ml of vehicle (phosphate buffered saline) via the tail vein at 1 and 6 h respectively post-CLP; (3) CLP + anti-CD123 group (n = 20): the rats underwent CLP, and 200ug (Weber et al., 2015) anti-CD123, diluted to 0.2 ml with phosphate buffered saline, was injected via the tail vein at 1 and 6 h respectively after CLP.

At 6 h post-CLP, all catheters were removed, all rats received a subcutaneous injection of Buprenorphine at a dose of 0.05 mg/kg for analgesia (repeated every 6 h for 2d), then were placed back in their cages where they had free access to water. Each group was then

randomly divided into three subgroups: 12 h, 24 h, and survival groups.

2.6. Measurements

All measurements were taken at baseline, 12, and 24 h post-operation. MAP was recorded on a monitor (BeneView T5, Mindary Bio-Medical Electronics Co. Ltd., Shenzhen, China). Arterial blood (0.1 ml) was drawn at baseline, 12, and 24 h post-operation. Arterial blood gas analyses (including PO_2/FiO_2 and arterial blood lactate) were performed with a Radiometer ABL FLEX™ 80 (Radiometer, Copenhagen, Denmark).

2.7. Serum biochemical assays

Blood samples were drawn through the PE-50 catheter using a sterile technique. After centrifugation (3000 × *g*, 10 min), the serum was separated and stored at −80 °C for further detection. Serum IL-1β (Abcam Biotech Co. Ltd., Cambridge, MA, USA), IL-3 (R&D Systems Biotech Co. Ltd., Emeryville, USA), IL-6 (Abcam Biotech Co. Ltd., Cambridge, MA, USA), IL-10 (Abcam Biotech Co. Ltd., Cambridge, MA, USA), and TNF-α (Abcam Biotech Co. Ltd., Cambridge, MA, USA) were detected using specific enzyme-linked immunoassay kits according to the manufacturer's instructions.

2.8. Sublingual microcirculation

In each group, sublingual microcirculation was visualized with the aid of a side stream dark-field imaging device (MicroScan; MicroVision Medical Inc., Amsterdam, Netherlands). The microcirculatory index, including total vessel density (TVD), perfused vessel density (PVD), the proportion of perfused vessels (PPV), and microvascular flow index (MFI) were measured and analyzed at baseline, 12, and 24 h post-operation. The image was divided into four quadrants, and the predominant type of flow (absent = 0, intermittent = 1, sluggish = 2, and normal = 3) was assessed in small vessels (less than 20 μm in diameter) in each quadrant. The MFI score represents the average value of the four quadrants (Boerma et al., 2005). PVD was calculated as the number of small perfused vessels crossing the lines, divided by the total length of the lines (De Backer et al., 2007; Yin et al., 2016). The vessel size was measured with a micrometer scale superimposed on the video display. All recordings were analyzed by two independent observers.

2.9. Western blot analysis and histological examination analysis

The rats' lungs were harvested after the operation in both the 12 and 24 h subgroups. The lung tissue was snap frozen in liquid nitrogen, pulverized, and then resuspended in ice-cold lysis buffer (Solarbio, Beijing, China). Protein concentrations were determined with the Bradford method. Lysates were allowed to solubilize on ice for 30 min, and particulate mass was removed by centrifugation at 15,000 × g for 15 min at 4 °C. Supernatants were analyzed by sodium dodecyl sulfate-polyacrylamide gel electrophoresis (SDS-PAGE). Primary antibodies used included rabbit anti-IL-3RB monoclonal antibody (1:400), rabbit anti-JAK2 monoclonal antibody (1:400), rabbit anti-SATA5 monoclonal antibody (1:400), and mouse anti-GAPDH monoclonal antibody (1:400), purchased from Abcam Biotech Co. Ltd. (Cambridge, MA, USA). Secondary antibodies were horseradish peroxidase-labeled antibodies (Thermo Scientific Pierce, Rockford, IL, USA). Blots were processed for enhanced chemifluorescence using a Pierce ECL Western blotting substrate (Thermo Scientific Pierce).

Lung and kidney tissues were harvested and immediately fixed in 10% formaldehyde, then paraffin-embedded and sliced at 12 and 24 h after the operation. The prepared tissue samples were stained with hematoxylin and eosin (HE) and observed under a light microscope for histological analysis. All slides were reviewed blindly and scored using a semiquantitative scoring system (Hou et al., 2009; Rezkalla et al., 1988; Yang et al., 2016). The severity of lung injuries was scored 0–4 based on the presence of edema, interstitial congestion, neutrophilic infiltrates, and cellular hyperplasia. The scoring was: 0, none; 1, less than 25%; 2, 25%–50%; 3, 51%–75%; and 4, more than 75%. The parameters for kidney injury were: tissue necrosis, loss of brush border in tubular epithelial cells, and formation of a tubular cast (Idrovo et al., 2012). The severity of kidney injury were scored, for each of the parameters, as: 0 (absent), 1 (a few), 2 (mild), 3 (moderate), to 4 (severe) (Wu et al., 2007). The histology injury scores were expressed as the sum of the individual scores.

2.10. 5-Day survival rate

In the survival subgroups within the three groups, census of animal behavior, vital parameters and survival were continuously examined and confirmed by two investigators at 1-hour intervals for a total of 5 days.

2.11. Statistical analysis

Statistical analyses were performed with SPSS 20.0 (SPSS Inc., Chicago, IL, USA). The data were expressed as mean ± SD. Least-Significant Difference *t*-test and ANOVA tests were used for the comparisons between two of the three groups. The Kaplan-Meier curve was used for survival analysis and log-rank test for differences between the two groups. $P < 0.05$ was considered statistically significant.

3. Results

3.1. Animal stratification and comparisons

A total of 55 rats were used in this study. Body weight, baseline hemodynamics, and blood analysis measurements did not differ significantly among the three groups (all $p > 0.05$) (Table 1).

There was a striking change in the weight, core temperature, $ETCO_2$, PaO_2/FiO_2, MAP, and lactate over time in the CLP group and the CLP + anti-CD123 group after the operation. Compared with the Sham group at the same time points, there was a significantly higher level of arterial blood lactate at 24 h post-CLP in the other two groups, and lower values of body weight, $ETCO_2$, MAP, and PO_2/FiO_2 at 24 h after CLP (all $p < 0.01$, Table 1). Markedly lower levels of lactate at 12 and 24 h post-CLP, yet higher core temperatures, $ETCO_2$, MAP, and PO_2/FiO_2 were observed in the CLP + anti-CD123 group at 24 h after CLP, in comparison with the CLP group (all $p < 0.01$, Table 1).

3.2. Inflammatory mediator and comparisons

There were higher levels of serum IL-3, TNF-α, IL-1β, IL-6, and IL-10 in the CLP group and the CLP + anti-CD123 group at 12 and 24 h after the operation, compared with the Sham group at the same time points (all $p < 0.01$, Fig. 1). Compared with the CLP group at the same time points, the serum levels of TNF-α, IL-1β, and IL-6 were significantly reduced at 12 and 24 h after CLP in the CLP + anti-CD123 group, (all $p < 0.01$, Fig. 1b–d). There were higher levels of IL-10 in the rat serum at 24 h after CLP in the CLP + anti-CD123 group ($p < 0.01$, Fig. 1e). However, the level of serum IL-3 did not change at the same time points between the CLP group and the CLP + anti-CD123 group ($p > 0.05$, Fig. 1a).

3.3. Anti-CD123 inhibits IL-3-triggered signal pathway in lungs

To clarify the effect of anti-CD123 on the expressed levels of phosphorylated IL-3 receptor β chain (p-IL-3RB), p-JAK2, and p-STAT5 proteins in lung tissue at 12 and 24 h post-CLP, the expressions of IL-3RB, p-IL-3RB, JAK2, p-JAK2, STAT5, and p-STAT5 proteins were each measured by western blotting. The expression levels of p-IL-3RB, p-

Table 1
Comparison of parameters in each group (mean ± SD).

Parameter	Time	Sham group	CLP group	CLP + anti-CD123 group
Body weight (g)	baseline	396.8 ± 9.0	397.6 ± 10.3	397.3 ± 8.9
	12 h	405.0 ± 1.7	404.8 ± 1.7	404.8 ± 1.9
	24 h	396.5 ± 14.3	382.6 ± 8.3*	380.7 ± 11.1*
Temperature	baseline	36.4 ± 0.2	36.4 ± 0.2	36.4 ± 0.1
(°C)	12 h	36.9 ± 0.2	35.4 ± 0.6*	36.9 ± 0.2#
	24 h	36.8 ± 0.2	33.6 ± 1.1*	37.9 ± 0.4*#
$ETCO_2$	baseline	41.9 ± 0.7	41.9 ± 0.7	42.0 ± 0.6
(mmHg)	12 h	40.6 ± 1.2	40.4 ± 1.6	40.6 ± 1.2
	24 h	42.8 ± 1.9	31.4 ± 2.0*	32.8 ± 2.4*#
PaO_2/FiO_2	baseline	438.5 ± 13.0	438.8 ± 12.0	440.3 ± 16.2
(mmHg)	12 h	420.8 ± 12.6	409.4 ± 36.6*	411.7 ± 32.0*
	24 h	451.7 ± 36.4	298.3 ± 51.4*	390.7 ± 39.1*#
MAP(mmHg)	baseline	98.2 ± 4.5	98.0 ± 4.3	97.2 ± 6.3
	12 h	94.9 ± 4.9	94.9 ± 6.1	95.8 ± 7.6
	24 h	96.4 ± 4.8	74.6 ± 3.9*	76.0 ± 8.5*#
Lac(mmol/L)	baseline	1.0 ± 0.3	0.9 ± 0.3	1.0 ± 0.3
	12 h	0.9 ± 0.1	2.2 ± 0.4*	1.1 ± 0.2#
	24 h	1.0 ± 0.2	3.3 ± 0.5*	2.2 ± 0.2*#

$ETCO_2$, end-tidal CO_2; PaO_2/FiO_2, oxygenation index; MAP, mean arterial pressure; Lac, arterial blood lactate; Sham group, animals were anesthetized and underwent laparotomy without puncture and cecal ligation(n = 15); CLP group, animals were anesthetized and underwent puncture and cecal ligation (n = 20); CLP + anti-CD123 group, animals were anesthetized and underwent puncture and cecal ligation with anti-CD123 injection(n = 20).*$p < 0.01$ vs. the sham group at the same point, #$p < 0.01$ vs. the CLP group at the same time points.

JAK2, and p-STAT5 proteins in lung tissue significantly increased after CLP stimulation ($p < 0.01$, Fig. 2a). However, compared with the CLP group at 12 and 24 h post-CLP, the protein levels of p-IL-3RB, p-JAK2, and p-STAT5 significantly decreased after the administration of anti-CD123 ($p < 0.01$, Fig. 2b).

3.4. Microcirculation changes after CLP

Sublingual microcirculatory flows were indistinguishable among the three groups at baseline (Fig. 3a), and there were no statistically significant changes in the Sham group over time (all $p > 0.05$, Fig. 3b). The sublingual microcirculatory flows exhibited progressive and striking decreases in the CLP and CLP + anti-CD123 groups at 12 and 24 h after the operation, and there was also a significant difference among the three groups (all $p < 0.01$, Fig. 3b). After administering anti-CD123, PVD, PPV, and MFI were significantly improved at 12 and 24 h in the CLP + anti-CD123 group, compared with the CLP group at the same time points (all $p < 0.01$, Fig. 3b).

3.5. Histopathological examination

In the CLP group, lung histopathology analysis showed alveolar

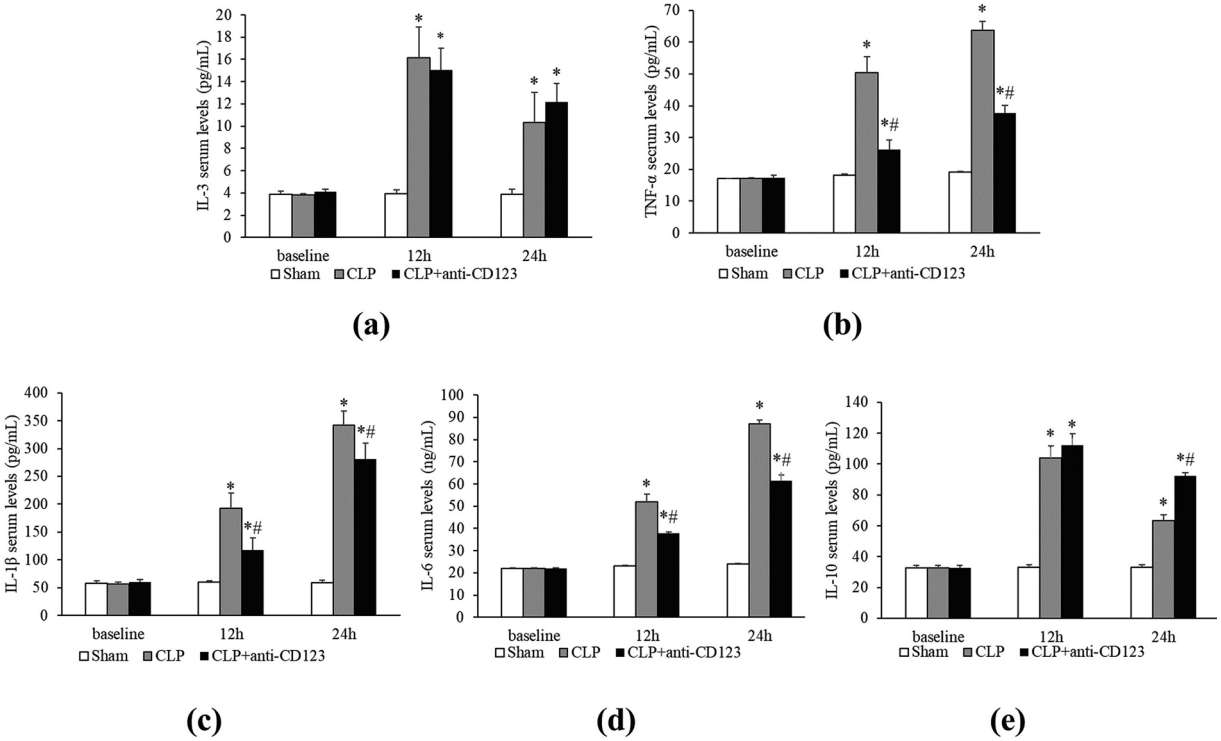

Fig. 1. Comparison of inflammatory markers in each group at different times. *$p < 0.01$ vs. Sham group at the same time points; #$p < 0.01$ vs. CLP group at the same time points.

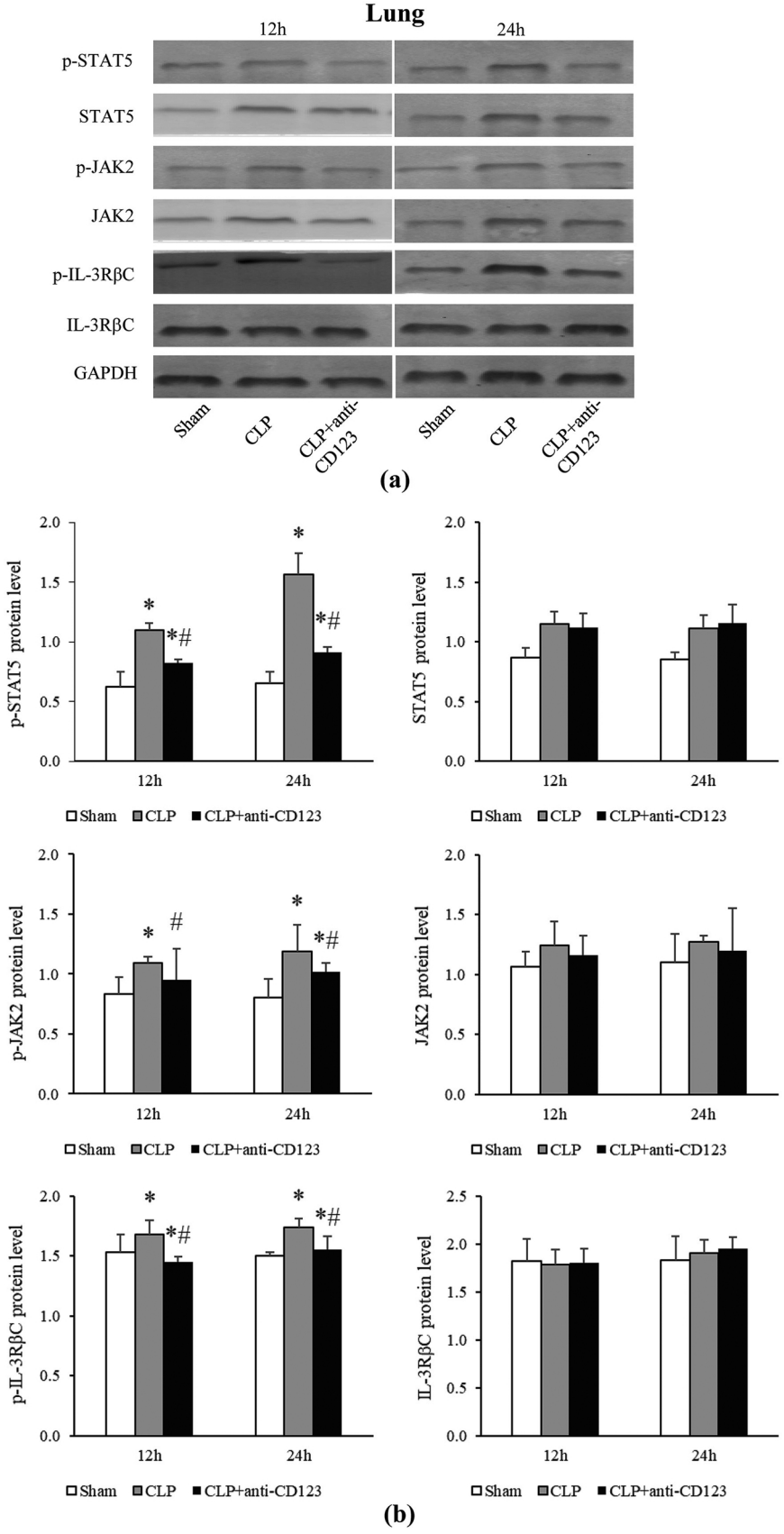

Fig. 2. (a) Administration of anti-CD123 reduced the expression levels of p-IL-3RB and p-STAT5 proteins at 12, 24 h post-CLP in lung tissue. Representative western blots show the levels of IL-3RB, p-IL-3RB, JAK2, p-JAK2, STAT5, and p-STAT5 proteins' expressions at 12, 24 h post-CLP in lung tissue in the three groups. (b) Administration of anti-CD123 reduced the expression levels of p-IL-3RB, p-JAK2 and p-STAT5 proteins at 12, 24 h post-CLP in lung tissue. Data are described as the mean ± SD of one experiment consisting of three replicates. Experiments were performed in triplicate. $^{*}p < 0.01$ vs. Sham group at the same point; $^{\#}p < 0.01$ vs. CLP group at the same point.

congestion and hyaline membrane formation, as well as neutrophil infiltration in the vessel walls. Renal sections revealed bleb formation and tubular luminal debris, and parenchymal cells demonstrated obvious vacuolization (Fig. 4a). However, there were moderate histological changes in the CLP + anti-CD123 group. Lower pathology scores, which represented less damage in the lung and kidney tissue,

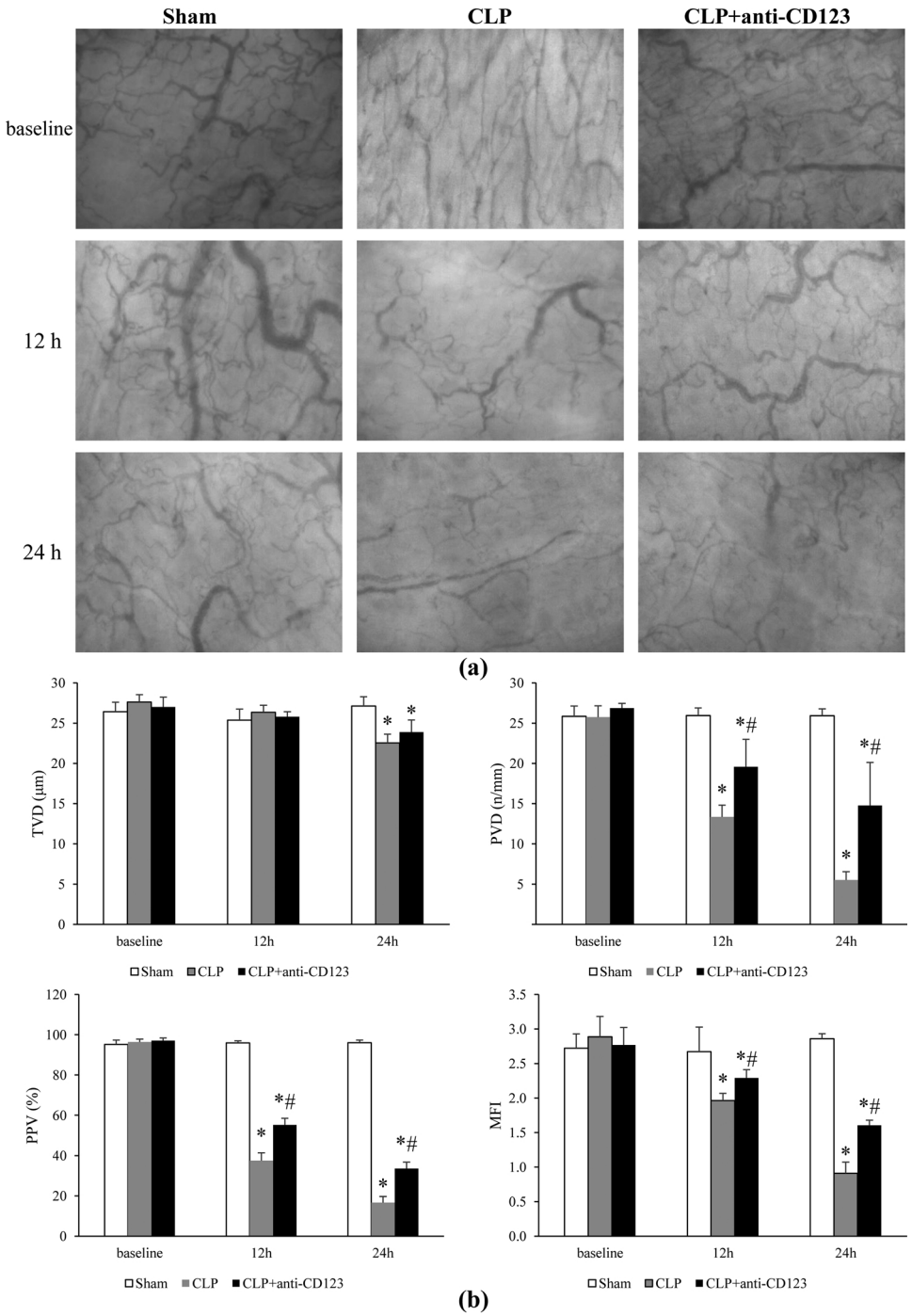

Fig. 3. (a) Images of sublingual microcirculation in the three groups. (b) The sublingual microcirculatory indexes PVD, PPV, and MFI of the CLP + anti-CD123 group at 12, 24 h after the operation were higher than the CLP group at the same time points, while the CLP group and the CLP + anti-CD123 group had lower TVD at 24 h post-CLP, PVD, PPV, and MFI at 12, 24 h post CLP compared with the Sham group. $^{*}p < 0.01$ vs. Sham group at the same time point; $^{\#}p < 0.01$ vs. CLP group at the same time point.

were observed in the CLP + anti-CD123 group compared with the CLP group (all $p < 0.01$, Fig. 4b).

3.6. Anti-CD123 decreases mortality in sepsis

Animals ($n = 5$ for Sham group, n = 10 for CLP group, and $n = 10$ for CLP + anti-CD123 group) were randomly grouped and monitored to assess the 5-day survival rate in each group. The results showed a clearly increased 5-day survival rate in the CLP + anti-CD123 group compared with the CLP group ($p < 0.01$, Fig. 4c).

4. Discussion

IL-3 binds to IL-3 receptor to promote inflammatory cell proliferation and differentiation via the IL-3-CD123-JAK2/STAT5 signaling pathway. JAK2/STAT5 is also an important pathway during sepsis (Cai et al., 2015). Blocking this pathway is therefore expected to affect the progression of sepsis. This study demonstrated that an IL-3 receptor antagonist, anti-CD123, may be a potential therapeutic target in the early stage of sepsis in a rat model induced by CLP.

In the current study, the administration of anti-CD123 resulted in

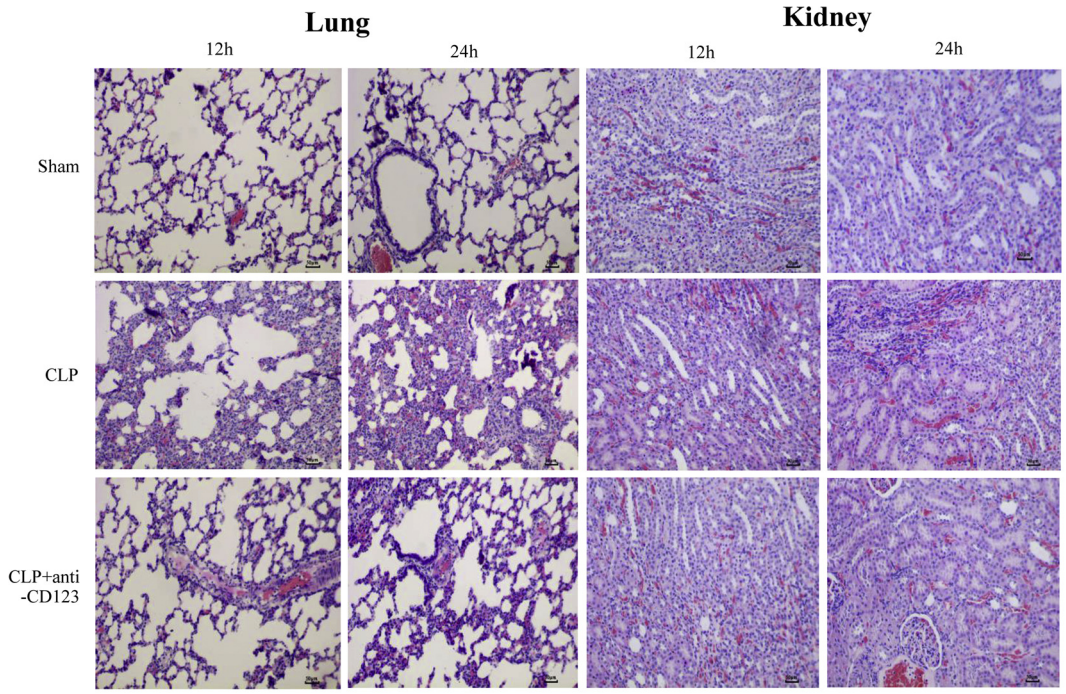

(a)

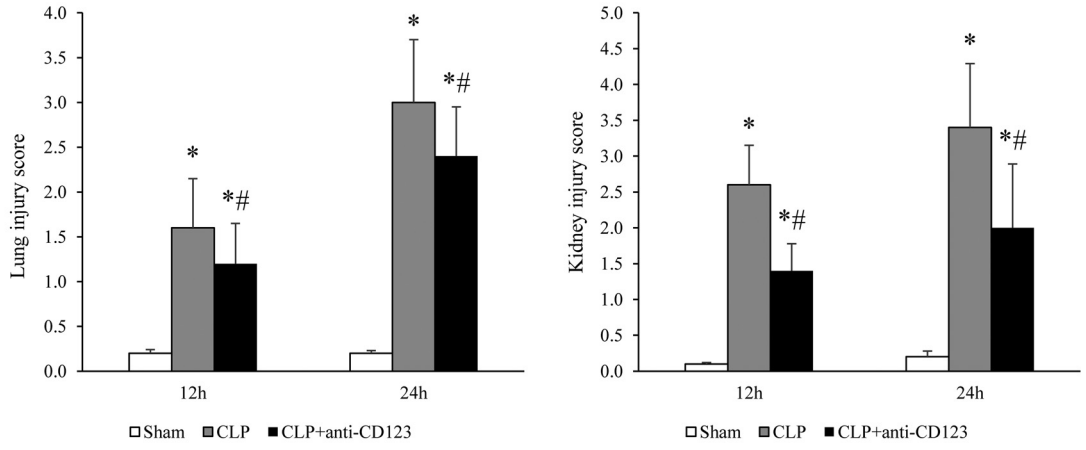

(b)

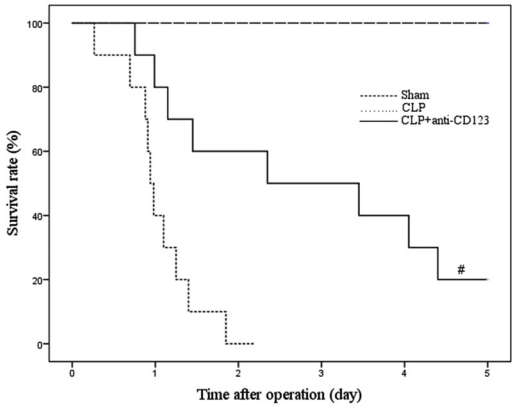

(c)

(caption on next page)

Fig. 4. (a) Anti-CD123 alleviated histopathology damage and organ dysfunction in the lungs and kidneys in CLP-induced sepsis in rats. The lung and kidney tissues were harvested at 12 h and 24 h after the operation. The tissue sections were stained with H&E. Original magnification 200 × . In the lung tissue, the inflammatory infiltration of neutrophils, macrophages, and plasma cells in the CLP group was more obvious than in the CLP + anti-CD123 group. In the kidney tissue, the rats in the CLP + anti-CD123 group had less inflammatory cell infiltration, necrosis, and degeneration. The figures were representative of at least three experiments performed on different experimental days. (b) Lower pathology scores, which represented more slight damage in lung and kidney tissue, were observed in the CLP + anti-CD123 group. $*p < 0.01$ vs. Sham group at the same time point; $^{\#}p < 0.01$ vs. CLP group at the same time point. (c) Kaplan-Meier survival curve for rats 5 days following the operation. Anti-CD123 improved the survival rate of rats in a sepsis model (Sham group, n = 5; CLP group, n = 10; CLP + anti-CD123 groups, n = 10); $\#p < 0.01$ vs. CLP group.

lower levels of arterial blood lactate, $ETCO_2$, MAP, and PO_2/FiO_2. However, due to the progression of sepsis caused by abdominal infection after surgery, and 12 h of fasting before surgery (Li et al., 2016), the rat weight loss in the anti-CD123 group and the CLP group. The reason was that CLP-induced mice weight would loss for the first 3 days (Hwang et al., 2019). Arterial blood lactate increased and $ETCO_2$ decreased in the anti-CD123 and CLP groups, which is consistent with the metabolic changes of sepsis. Studies have shown that CLP-induced sepsis causes an increase in lactate along with a decline in $ETCO_2$ 2 h post-CLP (Hua et al., 2018). Additionally, with the progresses of sepsis, MAP and sublingual microcirculation (PVD, PPV, and MFI) were also affected, and microcirculatory disorders lead to increase arterial blood lactate. MAP and ETCO2 have a high correlation, therefore ETCO2 declines with a decrease in MAP (Hua et al., 2018). Eventually, microcirculatory disorders can lead to organ injury and shorten survival time (Hawiger et al., 2015; Massey et al., 2018), however, there were more direct trends and outcomes observed in the present study's CLP group.

The role IL-3 plays in the progress of sepsis is not entirely clear. Activated T cells and innate response activator (IRA) B cells have been identified to produce IL-3 (Bentzer et al., 2016; Broughton et al., 2014; Chousterman and Swirski, 2015). It is currently believed that peritoneal B1a cells are activated by microbial pathogens and give rise to IL-3 + B cells in the red pulp of the spleen. IL-3 acts on hematopoietic stem and progenitor cells to promote the emergency generation of inflammatory leukocytes which are then released into circulation (Weber et al., 2015). This leads to an uncontrolled cytokine storm, multi-organ failure, septic shock, and death. IL-3 can trigger severe sepsis in vivo, and it is responsible for the cytokine storm by generating a large pool of cells that upon recognizing bacterial components, produce cytokines in larger quantities (Laupland et al., 2012). In our study, the results indicated that with the increase in serum IL-3, the accompanying serum levels of cytokines (IL-1β, TNF-α, IL-6, and IL-10) escalated in the CLP group. The mechanism may be that IL-3 combines with its receptor on the cell surface, such as multi-potential hematopoietic stem cells, neutrophils, eosinophils, megakaryocytes, macrophages, lymphoid, or erythroid cells, and activates its multiple signal transduction pathways, including JAK-STAT, mitogen-activated protein (MAP) kinases, protein kinase B (PKB/AKT), and anti-apoptotic pathways (Miyajima et al., 1992; Reddy et al., 2000; Shelburne et al., 2002). All the aforementioned pathways, including the JAK/STAT pathway, the MAP pathway, and the PKB/AKT pathway, play roles in this key function attributed to IL-3. The MAP kinases pathway regulates many important cell physiological/pathological processes such as cell growth, differentiation, stress adaptation to the environment, and inflammatory responses (Sun et al., 2015). STAT proteins also serve as substrates for MAP kinases. PKB/AKT, in response to IL-3 stimulation, has been observed in multiple cell lines and has contributed to the transmission of cell survival signals in response to IL-3 (Reddy et al., 2000). The anti-apoptotic pathway effect on IL-3 stimulation is its anti-apoptosis, or cell survival, function. The JAK-STAT pathway appears to be the pivotal mediator of cytokine signaling pathways (Ihle, 1995). In sepsis, the recruitment of pro-inflammatory intermediates leads to the phosphorylation of JAK/STAT, and the JAK/STAT pathway plays a critical role in inflammation (Hotchkiss et al., 2016). However, in the JAK2-STAT5 signal pathway, the upstream activation of kinase JAK2 and activator STAT5 are important mediators of cytokine signaling (Grimley et al., 1999). Therefore, blocking the IL-3 receptor can restrain the IL-3-JAK2-STAT5 signal pathway. In the process, anti-CD123 restrains the JAK2-STAT5 signal pathway by blocking phosphorylation of JAK2 and the STAT5 protein, and can reduce leucocyte cell production in the blood to control the excessive release of IL-1β, TNF-α, and IL-6 (Hotchkiss and Sherwood, 2015). Notably, IL-1β, TNF-α, and IL-6 are key pro-inflammatory cytokines in sepsis (Houschyar et al., 2017; Ulloa and Tracey, 2005).

Sepsis is a syndrome characterized by a dysregulated response of the host to invading pathogens which involves hemodynamic alterations that lead to microcirculation disturbances (De Backer et al., 2013; Top et al., 2011) and multiple life-threatening organ dysfunctions (Angus and van der Poll, 2013; Singer et al., 2016). Among the injured organs, the lung, due to its large area and rounded vascular system, accumulates a large number of activated neutrophils and monocytes, and becomes one of the most vulnerable organs in the early stages of sepsis (Czermak et al., 1999; Park et al., 2019). In the current study, we found that the phosphorylation level of IL-3 receptor β-chain was decreased after the introduction of the antagonistic IL-3 receptor; meanwhile, the expression levels of JAK2 and STAT5 phosphorylated proteins in lung tissue were also declining. These results demonstrate how anti-CD123 affected the JAK2-STAT5 signaling pathway in a septic rat. Therefore, anti-CD123 could reduce serum cytokines by restraining the JAK2-STAT5 signaling pathway in the development of sepsis. The inflammatory response to sepsis was alleviated after early intravenous administration of anti-CD123 in CLP-induced sepsis. The levels of IL-1β, TNF-α, and IL-6 fell more significantly in the early phase in the CLP + anti-CD123 group, compared with the CLP group 12 h after CLP. However, IL-10 levels rose in the CLP + anti-CD123 group 24 h after CLP, demonstrating a clear anti-inflammatory pattern. Our results were similar to the study of Lorigados et al. (2018), where they used bone marrow-derived mononuclear cells to treat CLP-induced sepsis, and the results indicated lower TNF-α and increased IL-10 concentrations in plasma 24 h after CLP. Those results indicate that a significant anti-inflammatory response was initiated 24 h post-CLP. Our results suggested that anti-CD123 can regulate early inflammation in sepsis. However, the specific mechanism of IL-10 elevation is unclear.

As previously mentioned, microcirculation disorders play an important role in the development of sepsis (Bakker, 2016), and result in dysfunction of vital organs and an increase in mortality. Our study showed that rats had different degrees of microcirculation disturbances 12 h post-CLP. We found that the PVD (12 h: 19.58 ± 0.42 vs. 13.36 ± 1.45; 24 h: 14.76 ± 5.37 vs. 5.54 ± 0.10 n/mm), PPV (12 h: 55.25 ± 3.30% vs. 37.51 ± 3.82%; 24 h: 33.54 ± 3.17% vs. 16.63 ± 3.01%), and MFI (12 h: 2.29 ± 0.12 vs. 1.96 ± 0.10; 24 h: 1.61 ± 0.07 vs. 0.91 ± 0.16) of sublingual microcirculation were significantly higher in the CLP + anti-CD123 group than the CLP group at 12 and 24 h post-CLP. Hua et al. (Hua et al., 2018) demonstrated that the buccal PVD was significantly reduced from 5.60 ± 0.28 to 4.32 ± 0.44 n/mm and MFI from 3.00 ± 0.00 to 2.64 ± 0.15 at 2 h post-CLP in the CLP group. The difference between the PVD value in the two studies is related to different methods of microcirculation monitoring (sublingual and buccal mucosal). At the same time, the pathological sections of the lungs of the CLP group showed obvious alveolar septal thickening and destruction, and numerous inflammatory cells

accumulated in the alveoli. Histopathological analysis of kidney tissue showed glomerular swelling and inflammatory cells around them, but there were substantially less inflammatory cells in the CLP + anti-CD123 group than in the CLP group. We speculate that IL-3 may accelerate the proliferation of inflammatory cells and cause microcirculatory disorders leading to lung and kidney injuries. Additionally, the survival time of the rats was significantly longer in the CLP + anti-CD123 group than the CLP group (73.4 h and 27.3 h, respectively). The close relationship between the degree of microcirculatory disturbance and organ structure and function would directly affect the survival rate of rats. Sepsis has been defined as a severe endothelial dysfunction syndrome in response to intravascular and extravascular infections, leading to reversible or irreversible injury to microcirculation responsible for multiple organ failures (Hawiger and Musser, 2011). However, it is the number and severity of organ injuries that are directly related to mortality (Singer et al., 2016). In clinical research, patients whose IL-3 plasma levels were > 87.4 pg/ml during the first 24 h after the onset of sepsis had a poor outcome (Weber et al., 2015). Another clinical research study showed that high plasma IL-3 levels are associated with a high rate of organ failure and thus a greater risk of mortality, confirming the potential of IL-3 as an early diagnostic biomarker (Min et al., 2018). In our study, anti-CD123 blocked the role of IL-3 in the early stage of sepsis, inhibiting inflammatory storms, reducing organ damage severity, and prolonging survival time. Clinically, the drug that antagonizes the IL-3 receptor is CSL362 (produced by CSL Limited). It is a humanized IL-3-neutralizing monoclonal antibody drug that treats acute myeloid leukemia by antagonizing CD123, and research has been mainly focused on treating blood diseases. CSL362 blocks IL3 function through both IL-3Rα conformations via distinct and unexpected mechanisms, resulting in enhanced antibody-dependent cell-mediated cytotoxicity (ADCC) activity (Busfield et al., 2014). Currently, the drug has finished the first and second phases of its trial, and is now undergoing clinical trials (ClinicalTrial.gov Identifier: NCT01632852). CSL362 has broad prospects for treating blood diseases, and it is showing promising application prospects. Other clinical trials which used CSL362 have also made some progress in human blood diseases, such as myeloid leukemia (Lee et al., 2015; Nievergall et al., 2014; Xie et al., 2017) and systemic lupus erythematosus (Oon et al., 2016). These studies highlight the potential in the results of our animal experiment, where anti-CD123 inhibited the biological activity of IL-3 to treat early sepsis. While it may be a promising tool in the treatment of sepsis patients, more research and clinical experiments need to be conducted.

5. Limitations

There are several limitations of this study that are inherent in the use of an animal model of CLP-induced sepsis. First, blood sample collections were limited by using the rat model. Second, the measurements of microcirculation parameters in this study were semi-quantitative. Third, we used a high grade sepsis model, which may progress faster than some sepsis cases, and there are differences between animal models and actual clinical patients. For our research purposes, only an antibody treatment was performed and the rats were not treated in strict accordance with a routine sepsis bundle (Rhodes et al., 2017). We did not use antibiotics in this study to avoid interfering with the effect of anti-CD123 on inflammatory cytokines and organ function. Fourth, variations on the dose and timing of anti-CD123 administration have not yet been explored thoroughly; the drug anti-CD123 requires more clinical experiments to confirm its effect. Further study is required to determine the appropriate standardized application to sepsis.

6. Conclusion

Anti-CD123 can inhibit the physiological function of IL-3 to reduce early sepsis inflammatory factors, improve microcirculation, ameliorate organ function, and prolong survival time. Anti-CD123 may be a potential new treatment method for early sepsis.

Declarations of conflicts of interest

None.

Funding

This study was supported by a research grant from project of Leading Talents in Pearl River Talent Plan of Guangdong Province (No. 81000-42020004) and Guangzhou Science and Technology Plan (No. 201804010471).

References

Angus, D.C., van der Poll, T., 2013. Severe sepsis and septic shock. N. Engl. J. Med. 369, 840–851.
Bakker, J., 2016. Lactate levels and hemodynamic coherence in acute circulatory failure. Best Pract. Res. Clin. Anaesthesiol. 30, 523–530.
Bentzer, P., Fjell, C., Walley, K.R., et al., 2016. Plasma cytokine levels predict response to corticosteroids in septic shock. Intensive Care Med. 42, 1970–1979.
Boerma, E.C., Mathura, K.R., van der Voort, P.H., et al., 2005. Quantifying bedside-derived imaging of microcirculatory abnormalities in septic patients: a prospective validation study. Crit. Care 9, R601–606.
Briscoe, J., Kohlhuber, F., Muller, M., 1996. Jaks and stats branch out. Trends Cell Biol. 6, 336–340.
Broughton, S.E., Hercus, T.R., Hardy, M.P., et al., 2014. Dual mechanism of interleukin-3 receptor blockade by an anti-cancer antibody. Cell Rep. 8, 410–419.
Busfield, S.J., Biondo, M., Wong, M., et al., 2014. Targeting of acute myeloid leukemia in vitro and in vivo with an anti-cd123 mab engineered for optimal adcc. Leukemia 28, 2213–2221.
Cai, B., Cai, J.P., Luo, Y.L., et al., 2015. The specific roles of jak/stat signaling pathway in sepsis. Inflammation 38, 1599–1608.
Chousterman, B.G., Swirski, F.K., 2015. Innate response activator b cells: origins and functions. Int. Immunol. 27, 537–541.
Czermak, B.J., Breckwoldt, M., Ravage, Z.B., et al., 1999. Mechanisms of enhanced lung injury during sepsis. Am. J. Pathol. 154, 1057–1065.
De Backer, D., Hollenberg, S., Boerma, C., et al., 2007. How to evaluate the microcirculation: report of a round table conference. Crit. Care 11, R101.
De Backer, D., Donadello, K., Sakr, Y., et al., 2013. Microcirculatory alterations in patients with severe sepsis: impact of time of assessment and relationship with outcome. Crit. Care Med. 41, 791–799.
Deutschman, C.S., Tracey, K.J., 2014. Sepsis: current dogma and new perspectives. Immunity 40, 463–475.
Duronio, V., Clark-Lewis, I., Federsppiel, B., et al., 1992. Tyrosine phosphorylation of receptor beta subunits and common substrates in response to interleukin-3 and granulocyte-macrophage colony-stimulating factor. J. Biol. Chem. 267, 21856–21863.
Fleischmann, C., Scherag, A., Adhikari, N.K., et al., 2016. Assessment of global incidence and mortality of hospital-treated sepsis. Current estimates and limitations. Am. J. Respir. Crit. Care Med. 193, 259–272.
Grimley, P.M., Dong, F., Rui, H., 1999. Stat5a and stat5b: fraternal twins of signal transduction and transcriptional activation. Cytokine Growth Factor Rev. 10, 131–157.
Hawiger, J., Musser, J.M., 2011. How to approach genome wars in sepsis? Crit. Care 15, 1007.
Hawiger, J., Veach, R.A., Zienkiewicz, J., 2015. New paradigms in sepsis: from prevention to protection of failing microcirculation. J. Thromb. Haemost. 13, 1743–1756.
Hotchkiss, R.S., Sherwood, E.R., 2015. Immunology. Getting sepsis therapy right. Science 347, 1201–1202.
Hotchkiss, R.S., Monneret, G., Payen, D., 2013. Sepsis-induced immunosuppression: from cellular dysfunctions to immunotherapy. Nat. Rev. Immunol. 13, 862–874.
Hotchkiss, R.S., Moldawer, L.L., Opal, S.M., et al., 2016. Sepsis and septic shock. Nat. Rev. Dis. Primers 2, 16045.
Hou, L., Xie, K., Li, N., et al., 2009. 100% oxygen inhalation protects against Zymosan-induced sterile sepsis in mice: the roles of inflammatory cytokines and antioxidant enzymes. Shock 32, 451–461.
Houschyar, K.S., Pyles, M.N., Rein, S., et al., 2017. Continuous hemoadsorption with a cytokine adsorber during sepsis - a review of the literature. Int. J. Artif. Organs 40, 205–211.
Hua, T., Wu, X., Wang, W., et al., 2018. Micro- and macrocirculatory changes during sepsis and septic shock in a rat model. Shock 49, 591–595.
Hwang, J.S., Kim, K.H., Park, J., et al., 2019. Glucosamine improves survival in a mouse model of sepsis and attenuates sepsis-induced lung injury and inflammation. J. Biol. Chem. 294, 608–622.
Idrovo, J.P., Yang, W.L., Nicastro, J., et al., 2012. Stimulation of carnitine palmitoyltransferase 1 improves renal function and attenuates tissue damage after ischemia/reperfusion. J. Surg. Res. 177, 157–164.
Ihle, J.N., 1995. Cytokine receptor signalling. Nature 377, 591–594.
Ihle, J.N., 1996. Stats: signal transducers and activators of transcription. Cell 84,

331–334.
Kaukonen, K.M., Bailey, M., Suzuki, S., et al., 2014. Mortality related to severe sepsis and septic shock among critically ill patients in australia and new zealand, 2000-2012. JAMA 311, 1308–1316.
Laupland, K.B., Zahar, J.R., Adrie, C., et al., 2012. Severe hypothermia increases the risk for intensive care unit-acquired infection. Clin. Infect. Dis. 54, 1064–1070.
Lee, E.M., Yee, D., Busfield, S.J., et al., 2015. Efficacy of an fc-modified anti-cd123 antibody (csl362) combined with chemotherapy in xenograft models of acute myelogenous leukemia in immunodeficient mice. Haematologica 100, 914–926.
Leslie, K.B., Jalbert, S., Orban, P., et al., 1996. Genetic basis of hypo-responsiveness of a/j mice to interleukin-3. Blood 87, 3186–3194.
Li, A., Li, J., Bao, Y., et al., 2016. Xuebijing injection alleviates cytokine-induced inflammatory liver injury in clp-induced septic rats through induction of suppressor of cytokine signaling 1. Exp. Ther. Med. 12, 1531–1536.
Lorigados, C.B., Ariga, S.K.K., Lima, T.M., et al., 2018. Bone marrow cells transplant in septic mice modulates systemic inflammatory response via cell-cell contact. Shock.
Massey, M.J., Hou, P.C., Filbin, M., et al., 2018. Microcirculatory perfusion disturbances in septic shock: results from the process trial. Crit Care 22, 308.
Min, J., Nothing, M., Coble, B., et al., 2018. Integrated biosensor for rapid and point-of-care sepsis diagnosis. ACS Nano 12, 3378–3384.
Miyajima, A., Kitamura, T., Harada, N., et al., 1992. Cytokine receptors and signal transduction. Annu. Rev. Immunol. 10, 295–331.
Nievergall, E., Ramshaw, H.S., Yong, A.S., et al., 2014. Monoclonal antibody targeting of il-3 receptor alpha with csl362 effectively depletes cml progenitor and stem cells. Blood 123, 1218–1228.
O'Farrell, A.M., Ichihara, M., Mui, A.L., et al., 1996. Signaling pathways activated in a unique mast cell line where interleukin-3 supports survival and stem cell factor is required for a proliferative response. Blood 87, 3655–3668.
Oon, S., Huynh, H., Tai, T.Y., et al., 2016. A cytotoxic anti-il-3ralpha antibody targets key cells and cytokines implicated in systemic lupus erythematosus. JCI Insight 1, e86131.
Park, I., Kim, M., Choe, K., et al., 2019. Neutrophils disturb pulmonary microcirculation in sepsis-induced acute lung injury. Eur. Respir. J.
Reddy, E.P., Korapati, A., Chaturvedi, P., et al., 2000. Il-3 signaling and the role of src kinases, jaks and stats: a covert liaison unveiled. Oncogene 19, 2532–2547.
Rezkalla, S., Kloner, R.A., Khatib, G., et al., 1988. Effect of metoprolol in acute coxsackie virus b3 murine myocarditis. J. Am. Coll. Cardiol. 12, 412–414.
Rhodes, A., Evans, L.E., Alhazzani, W., et al., 2017. Surviving sepsis campaign: international guidelines for management of sepsis and septic shock: 2016. Intensive Care Med. 43, 304–377.
Rittirsch, D., Huber-Lang, M.S., Flierl, M.A., et al., 2009. Immunodesign of experimental sepsis by cecal ligation and puncture. Nat. Protoc. 4, 31–36.
Schindler, C., Darnell Jr., J.E., 1995. Transcriptional responses to polypeptide ligands: the jak-stat pathway. Annu. Rev. Biochem. 64, 621–651.
Shankar-Hari, M., Deutschman, C.S., Singer, M., 2015. Do we need a new definition of sepsis? Intensive Care Med. 41, 909–911.
Shelburne, C.P., McCoy, M.E., Piekorz, R., et al., 2002. Stat5: an essential regulator of mast cell biology. Mol. Immunol. 38, 1187–1191.
Silvennoinen, O., Witthuhn, B.A., Quelle, F.W., et al., 1993. Structure of the murine jak2 protein-tyrosine kinase and its role in interleukin 3 signal transduction. Proc. Natl. Acad. Sci. U. S. A. 90, 8429–8433.
Singer, M., Deutschman, C.S., Seymour, C.W., et al., 2016. The third international consensus definitions for sepsis and septic shock (sepsis-3). JAMA 315, 801–810.
Sun, Y., Liu, W.Z., Liu, T., et al., 2015. Signaling pathway of mapk/erk in cell proliferation, differentiation, migration, senescence and apoptosis. J. Recept. Signal Transduct. Res. 35, 600–604.
Top, A.P., Ince, C., de Meij, N., et al., 2011. Persistent low microcirculatory vessel density in nonsurvivors of sepsis in pediatric intensive care. Crit. Care Med. 39, 8–13.
Ulloa, L., Tracey, K.J., 2005. The "cytokine profile": a code for sepsis. Trends Mol. Med. 11, 56–63.
Weber, G.F., Chousterman, B.G., He, S., et al., 2015. Interleukin-3 amplifies acute inflammation and is a potential therapeutic target in sepsis. Science 347, 1260–1265.
Williams, G.T., Smith, C.A., Spooncer, E., et al., 1990. Haemopoietic colony stimulating factors promote cell survival by suppressing apoptosis. Nature 343, 76–79.
Wu, R., Dong, W., Zhou, M., et al., 2007. Ghrelin attenuates sepsis-induced acute lung injury and mortality in rats. Am. J. Respir. Crit. Care Med. 176, 805–813.
Xie, L.H., Biondo, M., Busfield, S.J., et al., 2017. Cd123 target validation and preclinical evaluation of adcc activity of anti-cd123 antibody csl362 in combination with nks from aml patients in remission. Blood Cancer J. 7, e567.
Yang, Y.C., Ciarletta, A.B., Temple, P.A., et al., 1986. Human il-3 (multi-csf): identification by expression cloning of a novel hematopoietic growth factor related to murine il-3. Cell 47, 3–10.
Yang, W.L., Ma, G., Zhou, M., et al., 2016. Combined administration of human ghrelin and human growth hormone attenuates organ injury and improves survival in aged septic rats. Mol. Med.
Yi, T., Mui, A.L., Krystal, G., et al., 1993. Hematopoietic cell phosphatase associates with the interleukin-3 (il-3) receptor beta chain and down-regulates il-3-induced tyrosine phosphorylation and mitogenesis. Mol. Cell. Biol. 13, 7577–7586.
Yin, L., Yang, Z., Yu, H., et al., 2016. Changes in sublingual microcirculation is closely related with that of bulbar conjunctival microcirculation in a rat model of cardiac arrest. Shock 45, 428–433.